Analysis of Land Use And Land Cover Changes In Madurai City Using EBBO- SVM Model

P.Dolphin devi
Part-Time Research Scholar, Dept of Computer Science
School of Information Technology, Madurai Kamaraj University, Madurai.

ABSTRACT

Land use and land cover change research has been connected to landslides, disintegration, land arranging and worldwide change. In light of the EBBO-SVM model, this examination predicts the spatial examples of land use in span of year dependent on the dynamic changes in land use examples utilizing remote detecting and geographic data framework. Agricultural exercises have been causing changes on the landscape bringing about transformation of land cover/use classes as well as varieties in agricultural land designs. Madurai city of India has encountered huge land cover/utilization changes for the most part because of changes in agricultural practices in the most recent decade. The principle target of the present is to investigate and distinguish the features and degree of land use and land cover changes in Madurai city in the previous 22 years and to recognize the fundamental powers behind the changes. EBBO-SVM model coordinates the upsides of SVM classifier and PCA with HOG investigation to anticipate future land use patterns dependent on investigations of land use changes previously. Our outcomes demonstrate that agricultural lands have changed over times of span with explicit size of the entire examination region.

Keywords: Land use, Land cover, Classification, Madurai, EBBO, SVM, PCA, HOG

I.INTRODUCTION

Land use research programs at a worldwide scale have turned out to be vital to universal atmosphere and ecological change inquire about since the dispatch of land use and land cover (LULC) change venture [1]. LULC has two separate phrasings that are frequently used reciprocally [2]. Land cover alludes to the biophysical attributes of earth's surface, including the conveyance of vegetation, water, soil, and other physical features of the land. While land use alludes to the manner by which land has been used by people and their territory, more often than not with an accentuation on the practical job of land for financial exercises [3–5]. For example, as far as urbanization, a lot of agricultural/forestry land has been changed into urban land, and mining exercises/oil misuse have happened worldwide to fulfill the needs of individuals and can straightforwardly and clearly lead to the LUCC[6, 7]. In past investigations, worldwide ecological changes, for example, discharges of greenhouse gases, worldwide environmental change, loss of biodiversity, and loss of soil assets have been firmly connected to LULC changes [8]. Land use and land cover change (LULCC) is the transformation of various land use types and is the aftereffect of complex cooperationsamong people and the physical condition t[9]. LULCC is a noteworthy driver of worldwide change and significantly affects environment forms, natural cycles and biodiversity [7, 10, 11]. In addition, LULCC is additionally firmly identified with the maintainable advancement of the social economy [12, 13]. Immense zones of the world's earthly surface have experienced LULCC [14–16]. With fast financial advancement, land uses change all the more quickly, and the difference among land use types additionally increments 17]. Different systems of LULC change discovery investigation were talked about by Lu et al [18]. It is conceivable to set up a model to anticipate the patterns in land uses in a specific timeframe through the investigation of past land use changes, which could give some premise to logical and compelling land use arranging, the board and natural reclamation in an examination region and direction for territorial financial improvement. Thusly, precise and state-of-the-art land cover change data is essential for comprehension and evaluating LULC changes. Remote detecting (RS) and geographic data framework (GIS) are basic devices in acquiring exact and timely spatial information of land use and land cover, just as breaking down the changes in an investigation area[19–21]. Remote detecting pictures can successfully record land use circumstances and give a brilliant wellspring of information, from which refreshed LULC data and changes can be removed, broke down and reproduced effectively through certain means[22, 23]. In this way, remote detecting is broadly used in the location and checking of land use at various scales[24–27]. GIS gives an adaptable situation to gathering, putting away, showing and investigating computerized information important for change detection[19, 28, 29].

II.RELATED WORK

Land cover change demonstrating means time addition or extrapolation when the displaying surpasses the known period[30]. Generally used models for evaluating land cover changes are diagnostic condition based models[31], factual models[32], developmental models[33], cell models[34], Markov models[35], cross breed models[36], master framework models[37] and multiagent models[38]. At present, the most generally used models in land use change observing and expectation are cell and operator based models or the blended model dependent on these two kinds of models[39–42]. The Markov chain and Cellular Automata (CA-Markov) model, one of a blended models, is the cross breed of the Cellular Automata and Markov models. This model adequately consolidates the benefits of the long haul expectations of the Markov model and the capacity of the Cellular Automata (CA) model to reproduce the spatial variety in a mind boggling framework, and this blended model can viably recreate land cover change[43]. A CA model is a dynamic model with nearby cooperations that mirror the advancement of a framework, where reality are considered as discrete units, and space is frequently spoken to as a normal cross section of two dimensions[44]. CA-based models have a solid capacity to speak to nonlinear, spatial and stochastic procedures. In any case, CA model can't speak to large scale social, monetary and social main impetuses that impact urban extension well. In this way, a mix of specialists into CA models results in the improved CA-Markov model[40]. In the Markov model, the adjustment in a zone is outlined by a progression of change probabilities starting with one state then onto the next over a predefined timeframe. These probabilities can be along these lines used to foresee the land use properties at explicit future time points[45]. The use of the CA-Markov model in LULCC studies has favorable circumstances, for example, its dynamic recreation capacity; high productivity with information, shortage and straightforward alignment; and capacity to mimic various land covers and complex patterns[17, 46]. Numerous analysts have connected the CA-Markov model to screen land use and landscape changes and predictions[23, 36, 47, 48]. Along these lines, we received this technique to acquire dependable outcomes for Jiangle. In this investigation, the 2025 and 2036 LULCs were anticipated dependent on the condition of 2003 and 2014 LULCs.

III. METHODOLOGY

Principal of the EBBO-SVM model land cover/use mapping is dependent on spatial, spectral and temporal interpretation on satellite imageries using pattern, tone, shape, size, texture, shadow and association of elements.

3.1Land Use Feature Extraction

Our proposed model was experimented by hybrid feature extraction of PHOG and Sparse PCA on satellite images and the short description as follows.

3.1.1 Sparse PCA

Regression form of Principle Component Analysis (PCA) is called sparse PCA. Consider a training sample of a given dataset as $X = \{x_i\}_{i=1}^{n}$ in R^p. Let assume the column of X are all zero. Singular Value Decomposition is used to decompose X in PCA.

$$X = UDV^T, \qquad (1)$$

Where
$Z = UD,$ Represents the principle components (PC's)
U = Eigen Matrix

This is to be noted that each important features of data can be represented by linear combination of p variables in each PC's. In [3] proposed a self-constrained regression criterion to derive PC's.
Let i^{th} row of the input matrix X, can be defined as x_i. Let $\alpha = [\alpha_1, \alpha_2, \ldots \alpha_k]^T$ and $\beta = [\beta_1, \beta_2, \ldots \beta_k]^T$.

For any $\lambda > 0$, let

$$(\hat{\alpha}, \hat{\beta}) = \arg\min_{\alpha,\beta} \sum_{i=1}^{n} \|x_i - \alpha\beta^T x_i\|^2 + \lambda \sum_{j=1}^{k} \|\beta_j\|^2 \qquad (2)$$

$subject\ to\ \|\alpha\|^2 = I_k.$

Then $\widehat{\beta_j} \propto V_j$ for j= 1,2,3,..k.
Sparse loading is obtained by adding lasso penalty into equation (2) , and these equations are optimized as

$$(\hat{\alpha},\hat{\beta}) = \arg\min_{\alpha,\beta}\sum_{i=1}^{n}\|x_i - \alpha\beta^T x_i\|^2 + \lambda\sum_{j=1}^{k}\|\beta_j\|^2 + \sum_{j=1}^{k}\lambda_{1,j}\,\|\beta_j\| \quad (3)$$

$$subject\ to\ \alpha^T\alpha = I_k.$$

Where the similar λ valus is used for all k components, $\lambda_{1,j}$ is permitted for correcting the value of j PCs. The above discussed optimization problem is an elastic net problem. By selecting suitable λ and $\lambda_{1,j,}$ we find sparse vector β_j. basically λ is selected to be a small positive number to overcome potential col-linearity problems in X . Assumed a fixed value of λ in Equation (3), can be solved by using the LARS-EN algorithm [26].

3.1.2 PHOG

In current evaluation, PHOG is used as a spatial based shape descriptor, which is applied on image for classification [27]. PHOG descriptor characterizes the spatial property of image edges and transformed it into vector. This descriptor is mostly stimulated by two bases: (1) pyramid representation [28], and (2) the Histogram of Oriented Gradients (HOG) [29].

In this research work, PHOG features are extracted from the edge of the land-use region. Here local features were taken by distributing edge orientation over an image and spatial details are extracted by tilting an image into sub region at various resolutions. . The procedures of extracting features from land-use region using PHOG are as follows.

Step 1: First, an input image is applied to edge detection process using canny edge detector. It represents the shape features of an image.

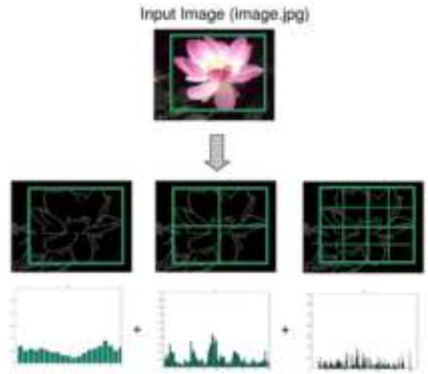

Fig 2: PHOG Feature extraction from an image

Step 2: Second, the image is divided into multiple pyramid level. As shown in Fig 2, the grid at level *"l"* has 2^l cells along every dimension.

Step 3: In each pyramid level of all grids has been undergone for HOF feature extraction process. Local shape features of an image can be represented by histogram function of all subregion. As mentioned in Step 1, Edge contours were computed and gradients of all regions have been estimated using Sobel Mask with size of 3 x 3 without Gaussian smoothing.

Step 4: Finally, the HOG vectors of all pyramid has been normalized and concatenated, which represents the spatial information of the input image. Also, different level of pyramid can be characterized by different size of vectors. That is level 0 is represented by a K vector based on K bins of the histogram. Similarly level 1 is represented by 4K v ector.

If the image is having the size of l then the PHOG descriptor based feature dimensionality is represented by

$$K\sum_{l=L} 4^l \quad (4)$$

3.2Land Cover Feature Extraction

3.21 EBBO algorithm

EBBO algorithm follows the migration and mutation phases to reach the global minima. It uses the same mutation approach as the BBO algorithm. Each solution has related mutation probability. The solutions with the lowest probability are more probable to mutate than the solutions with the highest probability. The mutation rate is inversely proportional to the probability of the solution. This prevents the dominance of the high probability solution. This approach encourages the mutation probability of poor solutions.

The proposed EBBO algorithm comprises three interesting features. Initially, the exploitation capability of the EBBO algorithm is high, as it follows the migration concept of the BBO algorithm. This could efficiently distribute the information between the solutions. Secondly, the mutation operator with minimum mutation probability maintains the exploration capability of the algorithm. Finally, the integration of the modified clear duplicate operator prevents the similar solutions and maintains the diversity between the population.

EBBO Algorithm

1: Initialize the population P randomly.
2: Evaluate the fitness for each individual in P
3: Sort the population from best to worst.
4: Initialize species count probability of each Habitat
5: While the termination criteria is not satisfied do
6: Save the best habitats (Elitism)
7: For each habitat, map the HSI to number of Species S
8: Compute λ and μ for each individual SIV
9: Probabilistically choose the immigration island based on immigration rates.
10: Migrate randomly selected SIVs based on the selected island in Step9.
11: Mutate the population probabilistic ally as per habitat mutation algorithm
12: Evaluate the fitness for each individual in P.
13: Sort the population from best to worst
14: Replace worst with best habitat from temporary
15: Check for feasibility of each individual SIV.
16: Check for similar habitat and replace similar habitat as per modified clear duplicate operator algorithm
17: end while

3.22 MDLTP and VAR for multispectral bands

The DLTP(Discrete Local Texture Pattern) operator for the gray scale image is expanded as Multivariate DLTP (MDLTP). Three suitable bands are selected among the multispectral bands for the classification of land cover. The selected bands are combined to form a Red, Green and Blue (RGB) image. Nine DLTP operators are computed in the RGB image. Among them, three DLTP operators individually define the local texture in each RGB band. Six DLTP operators define the local texture of the cross relationship of bands. The cross relationship is found by substituting the center pixel of the single band in its neighborhood along with the center pixel of additional band. Nine DLTP operators are organized in a 3×3 matrix. The MDLTP is estimated as follows by computing the DLTP for the 3×3 matrix

$$MDLTP = DLTP \begin{bmatrix} DLTP\ g_i^R, g_c^R & DLTP\ g_i^G, g_c^R & DLTP\ g_i^B, g_c^R \\ DLTP\ g_i^R, g_c^G & DLTP\ g_i^G, g_c^G & DLTP\ g_i^B, g_c^G \\ DLTP\ g_i^R, g_c^B & DLTP\ g_i^G, g_c^B & DLTP\ g_i^B, g_c^B \end{bmatrix} \quad (5)$$

Where 'i' represents the total number of pixels in 3×3 neighborhood. It ranges from 0 to 7.

The univariate variance measure (VAR) is prolonged as multivariate VAR (MVAR) for the remote sensed images. The separate independent variances $VAR_1, VAR_2\ and\ VAR_3$ of RGB bands are computed and combined into a distinct composite variance by using the formula described below

$$MVAR = \frac{1}{3}\sum_{i=1}^{3}(VAR_i - \mu_3)^2\ Where\ \mu_3 = \frac{1}{3}\sum_{i=1}^{3} VAR_i \quad (6)$$

3.3SVM classification

The SVM classifier can classify the non-linearly separable pixels. The support vectors are the samples that are located closer to the dividing hyperplane. The SVM orientates this hyperplane such that the hyperplane is located distant from the aspirants of both classes. The optimization problem of obtaining the support vectors with the highest margin about the separating hyperplane is resolved while subjecting to an acceptance value. The classifier solves the optimization problem using one of the kernels such as linear, Radial Basis Function (RBF), wavelet, sigmoid, polynomial and frame. The sign of the SVM output is evaluated to classify each new testing sample.

Multi-class classification is performed in the SVM algorithm while following two approaches such as one-on-one and one-on-all. In one-on-one approach, one SVM classifier is used per each pair of classes. The whole set of the patterns is simultaneously categorized into two classes. Finally, the patterns that are to be classified into multiple classes are fixed to a single class using the probability measures. The multiclass classification steps are described as follows

Training phase

- If 'n' represents the number of classes, then nC_2 SVMs are required.
- Each SVM algorithm is trained with the 2D histograms of well-recognized training samples and their class labels.

Testing phase

- The 2D global histogram of the unidentified sample is applied as input to all SVMs.
- The output of the SVM algorithm per pair of classes is plotted to a native probability value.

Then, the overall posterior probability is obtained from the distinct probabilities for decoding the class label of the unidentified sample.

IV. PERFORMANCE EVALUATION

Land use and land Cover in Madurai – 1994

Availability of Land sat imageries of the year 1996 fallow land covers above 46% of the study area.Build up land use in remaining 54% in Madurai city. Land use includes settlements, transportation and recreation places. In 2004, land use area is increased as 67%, which decrease the land cover as 33% in study image. The details are illustrated in Table 1.

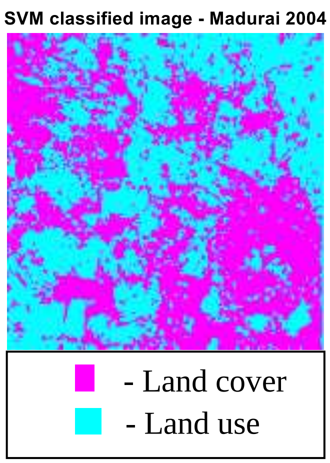

Fig 1 SVM based classifier image – Madurai 2004

Table 1 Land use and Land cover changes in Madurai

S.No	Madurai – 1996	Madurai - 2004
1	Land use – 54%	Land use – 67%
2	Land cover – 46%	Land cover – 33%

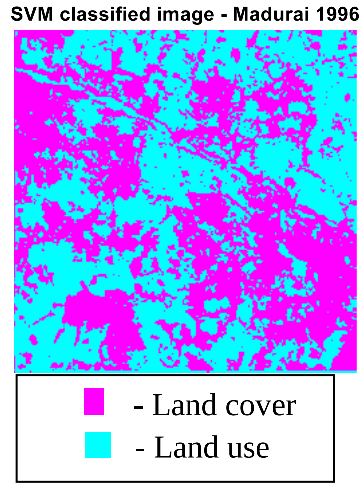

Fig 2 SVM based classifier image – Madurai 1996

V. CONCLUSION

The land use and land cover changes occurred in Madurai city between 1996 to 2014 using remote sensing image using EBBO-SVM model. The study has clearly brought to build up land the main city for urban& settlements in Madurai city. Any planning towards sustainable development should aim at preserving the land under cultivation. The study area under agriculture and water bodies change to build up areas highly. Land use and land cover mapping and detection of changes has shown here. It may not provide the ultimate explanation for all problems related to land use/ land cover changes but it serves as a base to understand the patterns and possible causes and consequences of land and land cover changes in the study area.

References

1. Han H, Yang C, Song J. Scenario Simulation and the Prediction of Land Use and Land Cover Change inBeijing, China. Sustainability-Basel. 2015; 7(4):4260–79. https://doi.org/10.3390/su7044260

2. Rawat JS, Kumar M. Monitoring land use/cover change using remote sensing and GIS techniques: Acase study of Hawalbagh block, district Almora, Uttarakhand, India. The Egyptian Journal of RemoteSensing and Space Science. 2015; 18(1):77–84. https://doi.org/10.1016/j.ejrs.2015.02.002.

3. McConnell WJ. Land Change: The Merger of Land Cover and Land use Dynamics A2—Wright, JamesD. International Encyclopedia of the Social & Behavioral Sciences (Second Edition). Oxford: Elsevier;2015. p. 220–3.

4. Lambin E. Land Cover Assessment and Monitoring. Encyclopedia of Analytical Chemistry: John Wiley& Sons, Ltd; 2006.

5. Arsanjani JJ. Dynamic Land Use / Cover Change Modelling :Geosimulation and Agent-Based Modelling. Vienna: University of Vienna; 2011.

6. Li L, Lu D, Kuang W. Examining Urban Impervious Surface Distribution and Its Dynamic Change inHangzhou Metropolis. Remote Sens-Basel.2016; 8(3). https://doi.org/10.3390/rs8030265

7. Basommi LP, Guan Q-f, Cheng D-d, Singh SK. Dynamics of land use change in a mining area: a casestudy of Nadowli District, Ghana. J Mt Sci. 2016; 13(4):633–42. https://doi.org/10.1007/s11629-015-3706-4

8. Li X, Wang Y, Li J, Lei B. Physical and Socioeconomic Driving Forces of Land-Use and Land-CoverChanges: A Case Study of Wuhan City, China. Discrete Dyn Nat Soc. 2016. https://doi.org/10.1155/2016/8061069

9. Pielke RA, Sr., Pitman A, Niyogi D, Mahmood R, McAlpine C, Hossain F, et al. Land use/land coverchanges and climate: modeling analysis and observational evidence. Wires Clim Change. 2011; 2(6):828–50. https://doi.org/10.1002/wcc.144

10. Verburg PH, Eck JRRv, NijsTCMd, Dijst MJ, Schot P. Determinants of Land-Use Change Patterns inthe Netherlands. Environ Plann B. 2004; 31(1):125–50. https://doi.org/10.1068/b307

11. Behera MD, Borate SN, Panda SN, Behera PR, Roy PS. Modelling and analyzing the watershed dynamics using Cellular Automata (CA)–Markov model–A geo-information based approach. J. Earth Syst. Sci.. 2012; 121(4):1011–24. https://doi.org/10.1007/s12040-012-0207-5

12. Yin J, Yin Z, Zhong H, Xu S, Hu X, Wang J, et al. Monitoring urban expansion and land use/land cover changes of Shanghai metropolitan area during the transitional economy (1979–2009) in China. Environ Monit Assess. 2011; 177(1–4):609–21. https://doi.org/10.1007/s10661-010-1660-8 PMID: 20824336

13. Caldas M, Walker R, Arima E, Perz S, Aldrich S, Simmons C. Theorizing Land Cover and Land Use Change: The Peasant Economy of Colonization in the Amazon Basin. Ann Assoc Am Geogr. 2007; 97 (1):86–110.

14. Galicia L, Garcia-Romero A. Land use and land cover change in highland temperate forests in the IztaPopo National Park, central Mexico. Mt Res Dev. 2007; 27(1):48–57. https://doi.org/10.1659/0276-4741(2007)27[48:lualcc]2.0.co;2

15. Scanlon BR, Reedy RC, Stonestrom DA, Prudic DE, Dennehy KF. Impact of land use and land cover change on groundwater recharge and quality in the southwestern US. Glob Change Biol. 2005; 11 (10):1577–93. https://doi.org/10.1111/j.1365-2486.2005.01026.x

16. Fox J, Vogler JB. Land-use and land-cover change in montane mainland southeast Asia. Environmental Management. 2005; 36(3):394–403. https://doi.org/10.1007/s00267-003-0288-7 PMID: 16132447

17. Hyandye C, Martz LW. A Markovian and cellular automata land-use change predictive model of the Usangu Catchment. Int J Remote Sens. 2017; 38(1):64–81. https://doi.org/10.1080/01431161.2016. 1259675

18. Lu D, Mausel P, Brondı ´zio E, Moran E. Change detection techniques. Int J Remote Sens. 2004; 25 (12):2365–401. https://doi.org/10.1080/0143116031000139863

19. Reis S. Analyzing Land Use/Land Cover Changes Using Remote Sensing and GIS in Rize, North-East Turkey. Sensors. 2008; 8(10):6188–202. https://doi.org/10.3390/s8106188 PMID: 27873865

20. Pervez W, Uddin V, Khan SA, Khan JA. Satellite-based land use mapping: comparative analysis of Landsat-8, Advanced Land Imager, and big data Hyperion imagery. J Appl Remote Sens. 2016; 10. https://doi.org/10.1117/1.jrs.10.026004

21. Srivastava PK, Singh SK, Gupta M, Thakur JK, Mukherjee S. Modeling Impact of Land Use Change Trajectories on Groundwater Quality Using Remote Sensing and GIS. Environ EngManag J. 2013; 12 (12):2343–55.

22. Pradhan B, Lee S, Mansor S, Buchroithner M, Jamaluddin N, Khujaimah Z. Utilization of optical remote sensing data and geographic information system tools for regional landslide hazard analysis by using binomial logistic regression model. J Appl Remote Sens. 2008; 2.https://doi.org/10.1117/1.3026536.

23. Singh SK, Laari PB, Mustak S, Srivastava PK, Szabo´ S. Modelling of land use land cover change using earth observation data-sets of Tons River Basin, Madhya Pradesh, India. Geocarto Int. 2017:1–34.

24. Hua AK. Land Use Land Cover Changes in Detection of Water Quality: A Study Based on Remote Sensing and Multivariate Statistics. Journal of environmental and public health. 2017; 2017:7515130-. https://doi.org/10.1155/2017/7515130 PMID: 28377790

25. Olokeogun OS, Iyiola K, Iyiola OF. Application of remote sensing and GIS in land use/land cover mapping and change detection in Shasha forest reserve, Nigeria. ISPRS—Int Arch Photogramm. 2014; XL-8(8):613–6.

26. Rai PK, Vishwakarma CA, Thakur S, Kamal V, Mukherjee S. Changing Land Trajectories: A Case Study from India Using a Remote Sensing Based Approach. European Journal of Geography. 2016; 7 (2):63–73.

27. Mishra VN, Rai PK, Kumar P, Prasad R. Evaluation of land use/land cover classification accuracy using multi-resolution remote sensing images.Forum geografic. 2016; XV(1):45–53. https://doi.org/10.5775/fg.2016.137.i

28. Khan S, Qasim S, Ambreen R, Syed ZUH. Spatio-Temporal Analysis of Landuse/Landcover Change of District Pishin Using Satellite Imagery and GIS.Journal of Geographic Information System. 2016; 8 (3):361–8.

29. Zeleke G, Hurni H. Implications of Land Use and Land Cover Dynamics for Mountain Resource Degradation in the Northwestern Ethiopian Highlands. Mt Res Dev. 2001; 21(2):184–91. https://doi.org/10.1659/0276-4741(2001)021[0184:IOLUAL]2.0.CO;2

30. Paegelow M, Olmedo MTC. Possibilities and limits of prospective GIS land cover modelling—a compared case study: Garrotxes (France) and Alta AlpujarraGranadina (Spain). Int J GeogrInf Sci. 2005; 19(6):697–722. https://doi.org/10.1080/13658810500076443

31. Shamsi SRF. Integrating Linear Programming and Analytical Hierarchical Processing in Raster-GIS to Optimize Land Use Pattern at Watershed Level.Journal of Applied Sciences and Environmental Management. 2010; 14(2):81–5.

32. Hyandye C. GIS and Logit Regression Model Applications in Land Use/Land Cover Change and Distribution in Usangu Catchment. American Journal of Remote Sensing 2015; 3(1):6–16.

33. Aitkenhead MJ, Aalders IH. Predicting land cover using GIS, Bayesian and evolutionary algorithm methods. J Environ Manage. 2009; 90(1):236–50. https://doi.org/10.1016/j.jenvman.2007.09.010 PMID: 18079039

34. Singh SK, Mustak S, Srivastava PK, Szabo´ S, Islam T. Predicting Spatial and Decadal LULC Changes Through Cellular Automata Markov Chain Models Using Earth Observation Datasets and Geo-information. Environmental Processes. 2015; 2(1):61–78.

35. Yang X, Zheng X-Q, Lv L-N. A spatiotemporal model of land use change based on ant colony optimization, Markov chain and cellular automata. Ecol Model. 2012; 233:11–9.https://doi.org/10.1016/j.ecolmodel.2012.03.011

36. Subedi P, Subedi K, Thapa B. Application of a Hybrid Cellular Automaton–Markov (CA-Markov) Model in Land-Use Change Prediction: A Case Study of Saddle Creek Drainage Basin, Florida. Science & Education. 2013; 1(6):126–32.

37. Stefanov WL, Ramsey MS, Christensen PR. Monitoring urban land cover change: An expert system approach to land cover classification of semiarid to arid urban centers. Remote Sens Environ. 2001; 77 (2):173–85.

38. Ralha CG, Abreu CG, Coelho CGC, Zaghetto A, Macchiavello B, Machado RB. A multi-agent model system for land-use change simulation. Remote Sens Environ. 2013; 42:30–46. https://doi.org/10.1016/j.envsoft.2012.12.003

39. Sohl TL, Claggett PR. Clarity versus complexity: Land-use modeling as a practical tool for decisionmakers. J Environ Manage. 2013; 129:235–43. https://doi.org/10.1016/j.jenvman.2013.07.027. https://doi.org/10.1016/j.jenvman.2013.07.027 PMID: 23954777

40. Zhao L, Peng Z-R. LandSys: an agent-based Cellular Automata model of land use change developed for transportation analysis. J TranspGeogr.2012; 25:35–49.

https://doi.org/10.1016/j.jtrangeo.2012.07.006.

41. Stevens D, Dragićević S. A GIS-Based Irregular Cellular Automata Model of Land-Use Change. Environ Plann B 2007; 34(4):708–24. https://doi.org/10.1068/b32098.

42. Myint SW, Wang L. Multicriteria decision approach for land use land cover change using Markov chain analysis and a cellular automata approach. Can J Remote Sens. 2006; 32(6):390–404. https://doi.org/10.5589/m06-032.

43. He D, Zhou J, Gao W, Guo H, Yu S, Liu Y. An integrated CA-markov model for dynamic simulation of land use change in Lake Dianchi watershed. Beijing DaxueXuebao (ZiranKexue Ban)/ActaScientiarumNaturaliumUniversitatisPekinensis. 2014; 50(6):1095–105.

44. He C, Okada N, Zhang Q, Shi P, Zhang J. Modeling urban expansion scenarios by coupling cellular automata model and system dynamic model in Beijing, China. ApplGeogr. 2006; 26(3):323–45. https://doi.org/10.1016/j.apgeog.2006.09.006.

45. Wu C-D, Cheng C-C, Lo H-C, Chen Y-K. Application of SEBAL and Markov Models for Future Stream Flow Simulation Through Remote Sensing. Water ResourManag. 2010; 24(14):3773–97. https://doi.org/10.1007/s11269-010-9633-9.

46. Memarian H, Balasundram SK, Talib JB, Sung CTB, Sood AM, Abbaspour K. Validation of CA-Markov for Simulation of Land Use and Cover Change in the Langat Basin, Malaysia. Journal of Geographic Information System. 2012; 4(6):542–54.

47. Rendana M, Rahim SA, Mohd RIW, Lihan T, Rahman ZA. CA-Markov for predicting land use changes in tropical catchment area: a case study in Cameron Highland, Malaysia. Journal of Applied Sciences. 2015; 15(4):689–95.

48. Nguyen TA, Le PMT, Pham TM, Hoang HTT, Nguyen MQ, Ta HQ, et al. Toward a sustainable city of tomorrow: a hybrid Markov–Cellular Automata modeling for urban landscape evolution in the Hanoi city(Vietnam) during 1990–2030. Environment, Development and Sustainability.2017. https://doi.org/10.1089/sus.2017.29092.aml